Appl. Phys. B 70, 821–831 (2000) / Digital Object Identifier (DOI) 10.1007/s003400000249

Applied Physics B
Lasers
and Optics

A phase-modulated interferometer for high-precision spectroscopy

A. Wicht[1], M. Müller[1], V. Quetschke[1], R.-H. Rinkleff[1], A. Rocco[2], K. Danzmann[1,2]

[1] Institut für Atom- und Molekülphysik, Abteilung Spektroskopie, Universität Hannover, Callinstr. 38, 30167 Hannover, Germany
(E-mail: wicht@pallas.amp.uni-hannover.de)
[2] Max-Planck-Institut für Quantenoptik, Außenstelle Hannover, Callinstr. 38, 30167 Hannover, Germany

Received: 4 October 1999/Revised version: 11 January 2000/Published online: 19 April 2000 –

Abstract. We present a novel spectroscopic method based on a phase-modulated interferometer which is suitable for the high-precision measurement of absorption and index of refraction profiles. A comparison with competing methods, that is with interferometry and FM spectroscopy, is given. The combination of these two methods, the phase-modulated interferometer, is shown to be best suited for experiments aiming at the realization of novel optical media, for example media exhibiting an ultra-large index of refraction or strong dispersion without absorption. The theory of operation and a theoretical and experimental signal-to-noise analysis are presented. Current detection limits for optical phase shift and relative absorption are $1.1 \times 10^{-5}\,\mathrm{rad}/\sqrt{\mathrm{Hz}}$ and $2 \times 10^{-5}/\sqrt{\mathrm{Hz}}$, respectively. We demonstrate the effectiveness of this novel technique by investigating the absorption and index of refraction profiles of the $4s^2\,{}^1S_0 \rightarrow 4s4p\,{}^1P_1$ resonance transition at 423 nm in calcium.

PACS: 07.65; 07.57.Pt; 32.70.Jz

Over the last years it has been shown both theoretically and experimentally that the optical properties of atoms and molecules can be "designed" simply by introducing atomic coherence or utilizing quantum interference. Examples are cancellation of absorption [1], enhancing the index of refraction and the dispersion [2–4] and the realization of ultra-large non-linearities without absorption [5]. These media provide a variety of new applications, such as an ultra-sensitive magnetometer [6] or high-finesse broadband optical cavities (white-light cavities [7]). For their realization, precise knowledge and control of the absorption coefficient and of the index of refraction of these media are necessary. Since it overcomes some of the problems related to competing spectroscopic methods while offering the potential for shot-noise-limited measurement of optical spectra, the novel spectroscopic method that we present in this paper is best suited for the measurement of these properties.

Among the large number of existing spectroscopic methods there are only two providing highly sensitive and simultaneous detection of the absorption and phase shift (index of refraction) which a "probe field" experiences as it passes through the medium under investigation. The first method is given by the category of phase and/or amplitude modulation techniques whereas the second is an interferometric method.

Based on the pioneering work of Bjorklund [9] phase modulation techniques in the optical domain have been used and optimized for about two decades [8]. By choosing the phase modulation index M and the modulation frequency ω_m one can distinguish between two distinct regimes of phase modulation spectroscopy. The *wavelength modulation spectroscopy* utilizes a large phase modulation index ($M \gg 1$) and a modulation frequency small compared to the width Γ of spectral feature under investigation: $M \times \omega_\mathrm{m} \ll \Gamma$. This method reveals only the derivative of the absorption with respect to the optical frequency and does practically not provide information about the index of refraction [10]. The second limiting case where $M \ll 1$ and a $\omega_\mathrm{m} \gg \Gamma$, is referred to as *frequency modulation spectroscopy* (FMS). For this case, only the carrier and the first-order modulation sidebands of the phase-modulated optical field have to be considered [10]. When passing through the sample, these three spectral components will experience a certain phase shift and damping, which can be described by a complex amplitude transmission coefficient $T_n = \mathrm{e}^{-\delta_n} \times \mathrm{e}^{\mathrm{i}\,\phi_n}$, where $n = -1, 0, +1$ designates the low-frequency, the carrier, and the high-frequency component, respectively. Assuming small variation of the absorption and the phase shift with frequency ($|\delta_n - \delta_{n+1}|$, $|\phi_n - \phi_{n+1}| \ll 1$), the beat signal at the modulation frequency detected with a fast photodiode takes the form [10]:

$$I_{\omega_\mathrm{m}}(t) \propto M\,(\delta_{-1} - \delta_{+1})\,\cos\omega_\mathrm{m} t + M\,(\phi_{-1} + \phi_{+1} - 2\phi_0)\,\sin\omega_\mathrm{m} t\,. \quad (1)$$

From (1) it follows that a simultaneous measurement of the phase shift $\phi(\omega)$ (index of refraction) and the absorption $\delta(\omega)$ can only be achieved when one of the sidebands is swept across the spectral feature of interest, with the carrier and the other sideband not experiencing any phase shift or damping at all. One of the most important features of FMS is the

fact that quantum-noise (shot-noise)-limited sensitivity can be achieved experimentally for both absorption and phase shift detection [11]: First, FMS has no background signal. In the case of vanishing absorption and phase shift there is no signal at the modulation frequency. Second, the information is contained in the high-frequency component of the photodiode signal. At high modulation frequencies, detector electronics noise, technical laser frequency, and power noise can be suppressed below the shot-noise level of the optical field. Furthermore, techniques have been developed to overcome those technical problems encountered in FMS one encounters when trying to achieve shot-noise-limited sensitivity (RAM [11], interference effects [12], drift of baseline: two-tone-FMS [13]). Even sub-shot-noise-limited sensitivity for absorption measurements has been achieved with amplitude-squeezed lasers [14]. FM-noise spectroscopy [15] provides FMS without the need of active phase modulation and is based on the intrinsic broadband frequency noise of diode lasers.

Schmidt et al. [16] used a Mach–Zehnder interferometer for the simultaneous detection of the absorption and of the index of refraction in a Λ-scheme in Cs, exhibiting strong positive dispersion without absorption. In the limit of perfect contrast, a perfectly balanced power beam splitter at the output of the interferometer, and two ideal photodiodes (unity quantum efficiency, identical transimpedance gain), the differential mode (balanced) output of the interferometer can provide shot-noise-limited phase shift sensitivity, if the interferometer is operated at a "half fringe". Here, "half fringe" describes the situation where, for a balanced output beam splitter, the signals from both of the outputs equal each other: $I_1 = I_2 = I_0/2$ (see below). However, the absorption measurement is based on directly detecting the transmitted power and will therefore not reach a sensitivity comparable to FMS. In addition, for certain reasons not connected to the interferometric technique, Schmidt and co-workers had to ensure that the laser power in both arms of the interferometer was the same. Hence, for a weak probe, the detected signal must be small and technical noise problems can arise.

Müller et al. [3] developed a common-path heterodyne interferometer for which both the reference and probe beam are separated not in space but in frequency. The setup can be interpreted in terms of an interferometer operated at the difference frequency (microwave range). This method shows some similarity to FMS in the limit of complete absorption of the non-probing sideband and can provide shot-noise-limited sensitivity for phase shift detection. However, as with the homodyne interferometer, the absorption is directly detected so that shot-noise-limited sensitivity can not be achieved for this quantity. Nevertheless, this method offers some advantages compared to ordinary FMS, since it is not limited to a small phase modulation index (i.e. small probe power). In this way one can avoid those problems that can arise from the interaction of the non-probing sideband or the higher order sidebands with the sample. In addition, it technically simplifies the setup in those cases where phase-locked lasers must be used: then, additional active phase modulation is obsolete.

Although all of the spectroscopic methods mentioned so far seem to be well suited for the simultaneous and highly sensitive detection of absorption and refractive index profiles, they do not meet all of the requirements for "designing" the optical properties of certain media. In order to discuss this in Sect. 1, we will define five requirements a convenient setup has to meet, we will briefly evaluate the spectroscopic methods mentioned above with respect to these requirements, and we will introduce the basic concept of the novel method discussed in this paper. In Sect. 2, a theoretical description of this novel method is developed. These results are used to investigate its sensitivity limit in Sect. 3. In Sect. 4 we give a description of technical details, we discuss the operation as an active null instrument, and present some experimental data on the sensitivity achieved so far. Finally, we demonstrate the performance of the novel method by spectroscopically investigating the Ca $4s^2\ {}^1S_0 \rightarrow 4s4p\ {}^1P_1$ transition.

1 Basics of the novel method

The spectroscopy requirements for realizing novel optical media differ from those given for laser stabilization, optical clocks, or molecular spectroscopy. Although especially for high-precision spectroscopy a detailed understanding of the absorption line shape is essential for determining the line center, it is mainly the exact knowledge about the transition frequency that provides the information about, for example the molecule. In contrast, the absorption and index of refraction *profiles* are of major interest for the design of the novel media mentioned above. A spectroscopic setup dedicated to the investigation of these novel media has to meet the following requirements:

(i) The spectroscopic method should allow the *simultaneous measurement* of the absorption coefficient and of the index of refraction, as both vary with frequency. In principle, one can derive one of these profiles from the other by applying the Kramers–Kronig relations [17]. However, these relations assume that either the absorption or the index of refraction is known for every frequency. This can be a problem for very complex spectra of molecules, for example.

(ii) The method should *avoid cross-talking* between the absorption and index of refraction signal. Cross-talking can play a role especially for spectroscopy within the very vicinity of a resonance, where the absorption signal reaches its maximum and the index of refraction signal (usually an optical phase shift) approaches zero.

(iii) The (classical) measurement must not modify the optical properties of the medium under investigation. The signal should carry information concerning the absorption and the index of refraction of the probe field only. This is of importance for FMS, as discussed below.

(iv) A good signal-to-noise ratio should be achievable even at low probe powers: for our purpose of realizing negative dispersion without absorption [4], a sensitivity of $10^{-5} - 10^{-6}$ for relative absorption and 10^{-5}–10^{-6} rad for optical phase shifts should be reached at probe power levels of $\approx 20\,\mu$W.

(v) Since it is the absolute value of the absorption coefficient and of the index of refraction that is to be determined, calibration of the signals should be simple, accurate, and reliable. In the ideal case, the calibration factor is a constant and does not depend on laser power etc. Actually, this is a question of convenience rather than a requirement. Still, it turns out to be an advantage of the novel

method presented here so that we may add this point to this list of aspects used to compare different spectroscopic methods.

We begin our discussion by evaluating FMS with respect to these requirements. It first should be emphasized that only FMS used in the way described above can provide information for both optical phase shifts and absorption, with shot-noise-limited sensitivity. This also includes the novel method presented here and is due to the fact that all but the FMS detects transmitted fields rather than the absorbed fields (i, iv). However, some problems arise when FMS is used for investigations on novel optical media such as those providing an enhanced index of refraction. To recognize this, we notice that (1) is valid only in the limit of small phase shift and small absorption. Taking into account higher order terms and assuming that only one FM sideband, for example $n = 1$, experiences some phase shift and absorption, (1) becomes

$$\begin{aligned} I_{\omega_\mathrm{m}}(t) \propto M \times & \left\{ -\delta_1 + \frac{1}{2}\left(\delta_1^2 - \phi_1^2\right) - \frac{1}{6}\delta_1^3 + \frac{1}{2}\phi_1^2\delta_1 + \dots \right\} \\ & \times \cos\omega_\mathrm{m} t \\ & + M \times \left\{ \phi_1 - \delta_1\phi_1 + \frac{1}{2}\delta_1^2\phi_1 - \frac{1}{6}\phi_1^3 + \dots \right\} \\ & \times \sin\omega_\mathrm{m} t \,. \end{aligned} \tag{2}$$

Hence, the second-order terms give rise to cross-talking effects and to non-linearities. For example, near points of vanishing absorption where the index of refraction and consequently the phase shift can be large for certain systems [2], the absorption signal will be masked completely by the phase shift. Additionally, for phase shifts approaching $\approx \pi/2$, the phase shift signal strongly becomes non-linear or even ambiguous. Therefore, (ii) will not be satisfied in general. Further, in FMS there are two optical fields used for optical phase referencing, that is the carrier ($n = 0$) and the second FM sideband ($n = -1$), which both pass the medium. If the modulation frequency ω_m is not sufficiently large, both of the reference fields will experience varying phase shifts and absorption during an experiment when the laser frequency or the modulation frequency is swept. Of course, this will introduce an error to the signal. Finally, to obtain a good signal-to-noise ratio, the carrier usually has to be strong. Again, if the modulation frequency is too small, the strong carrier will drive the atoms thus modifying the optical properties measured by the probe field. In this sense, the measurement itself modifies the sample and vice versa, so that it might be difficult to meet (iii). In principle, this additional interaction between the measurement device and the sample can be strongly reduced by increasing the modulation frequency. However, one may reach technical limits at a few tens of GHz, which still may not be enough for example for molecular spectroscopy. Further, cross-talking and non-linearity problems still maintain as they are not related to the value of the modulation frequency. In conclusion we find, that FMS might not be well suited for those investigations that focus on the realization of certain novel optical media.

The Mach–Zehnder interferometer used by Schmidt and co-workers [16] substantially fulfills all but the second to the last of these requirements. Cross-talking (ii) is avoided and the calibration factor (v) of the phase-shift signal is a constant, if the interferometer is operated as an active null instrument and the phase-shift signal is derived from the feedback signal of the servo loop stabilizing the interferometer to a "half fringe". Since the optical phase reference and the probe field are separated in space, the reference neither is affected by the medium nor modifies the absorption and the index of refraction of the sample (iii). However, to get a convenient signal-to-noise ratio at low probe power levels within the sample, a "high-power" reference has to be used. This can be realized by using a strongly unbalanced beam splitter at the input of the interferometer, passing almost all of the probe laser power to the reference arm. Of course, this strongly reduces the contrast of the interferometer and therefore introduces some difficulties in locking the apparatus exactly at the desired working point (at a "half fringe"). Problems arising from imperfect contrast, from a not perfectly balanced output beam splitter and from unbalanced photodetectors at the output of the interferometer will shift the locking point of the interferometer thus introducing cross-talking effects and changing the calibration factor. Therefore, an interferometer like the one used by Schmidt and co-workers usually will be operated with a balanced input beam splitter [18]. Consequently, this will cause some difficulties in reaching a good signal-to-noise ratio at low probe field powers (iv). Please note, that even in the case of a perfectly balanced input beam splitter it will take some effort to overcome the other problems mentioned above. Therefore, we conclude that it will be difficult to satisfy (iii) and (iv) under experimental conditions. Nevertheless, it should be emphasized that the interferometric setup – at least in principle – provides the possibility to achieve shot-noise-limited sensitivity for optical phase shift detection.

When compared to the Mach–Zehnder interferometer the heterodyne interferometer of Müller et al. [3] has three major advantages. First, it satisfies (iv), since a high-power optical local oscillator (LO) may be used to achieve a large signal even for a low-power probe field (iv). The principle of operation for phase shift detection is the same as for FMS, so that shot-noise-limited sensitivity may be achieved with respect to this quantity. Second, this heterodyne interferometer may be interpreted as an interferometer operated at microwave frequency ($\omega_\mathrm{LO} - \omega_\mathrm{probe} = 9.2\,\mathrm{GHz}$), thus reducing the strong demands for passive mechanical stability which have to be satisfied in the case of an optical interferometer. Third, the phase shift information is contained at microwave frequency so that the common problems connected with dc measurements are omitted. However, the problems arising with the heterodyne interferometer are nearly the same as with FMS. Cross-talking (ii) is not avoided, since the signal is proportional to the product of probe power transmission and the optical phase shift. Additionally, for large optical phase shifts (≈ 1 rad), the phase detection becomes non-linear, since the heterodyne interferometer can not be operated as an active null instrument. Further, (iii) only is fulfilled in parts. The strong optical field driving the atoms [3] also serves as the constant-frequency optical phase reference, thus the optical LO does not introduce *additional* modification of the optical properties of the medium. However, in the limit of a strong probe the phase and amplitude of the *reference* optical field will be modified when the probe field is tuned during an experiment, so that the reference field no longer may serve as

a phase reference. In general, satisfying (iii) turns out to be crucial for a setup where both the probe and the reference field pass the medium.

On one hand, the comparison of these methods clearly shows that an interferometric setup satisfies most of the requirements and is the only way to inherently fulfill (iii). However, the most severe problems related to the setup used by Schmidt et al. are due to the difficulties in locking the interferometer exactly at the working point (at a "half fringe"). On the other hand, FMS and the heterodyne interferometer tell us how to overcome this problem. Consequently, a combination of interferometry and of the phase modulation technique should unite the advantages of both while at the same time avoiding the problems related to each of them. How this is done is shown in Fig. 1. The setup consists of a Mach–Zehnder interferometer utilizing an electro-optic phase modulator within the reference arm. Although each single output provides full information about phase shifts and absorption and would allow locking the interferometer at a "dark fringe" or at a "half fringe" without any subtraction of a background signal, the differential mode signal (balanced signal) is detected for signal-to-noise reasons. By demodulating the signal at the modulation frequency or higher harmonics the phase shift and absorption can be determined. As we will see later on, this setup meets (i), although it is only the optical phase shift for which shot-noise-limited sensitivity can be achieved in principle. Since the setup can be operated as an active null instrument for phase shift detection, cross-talking and non-linearities present in FMS, for example, are avoided (ii). Further, calibration of the absorption signal is simple and the calibration factor for the phase shift measurement even is a constant determined by the half-wave voltage of the EOM (v). The optical phase reference does not pass the medium thus inherently omitting problems arising from the (classical) interaction between the apparatus and the sample under investigation (iii). The novel method makes use of the strong local oscillator concept known from FMS by using a strongly unbalanced input beam splitter (iv). In contrast to the standard Mach–Zehnder interferometer, this now does not introduce problems to actually lock the interferometer at the desired operating point ("half fringe" or "dark fringe"). Further, problems arising from a not perfectly balanced output beam splitter and from unbalanced photodetectors are omitted as well.

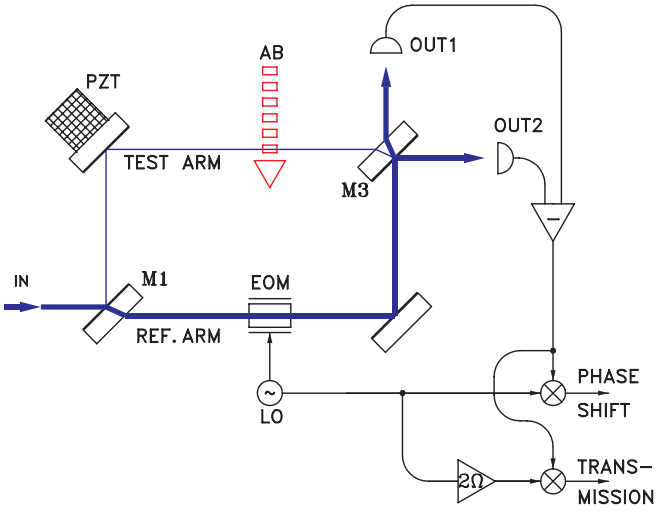

Fig. 1. Principle of operation of the novel method which consists of a combination of a Mach–Zehnder interferometer and FMS. The reference arm of the interferometer is phase modulated (EOM), whereas the test arm intersects a chopped atomic beam (AB). The differential mode signal (balanced output) of the interferometer provides the information about optical phase shifts and absorption. M1, M3: beam splitter, LO: local oscillator. A piezoelectric transducer (PZT) is used for optical phase correction

Of course, we do not gain these advantages for free. To see this, one should recognize that the setup could be interpreted as a FMS method, where the carrier ($n = 0$) serves as a probe and where strong sidebands spatially bypassing the interaction zone serve as the phase reference. Hence, from (1) it is obvious that only phase shifts can be detected with FMS methods and therefore may be measured with shot-noise-limited sensitivity. The absorption measurement is based on a detection of the transmitted field amplitude ("direct detection"). Therefore, the absorption sensitivity will always be limited by dc-power noise of the laser. Nevertheless, since the strong-LO concept can be applied to the absorption measurement, this method is superior to the direct detection of absorption by ordinary absorption spectroscopy, so that a good signal-to-noise ratio can be achieved even at low probe powers. Finally, as for the setup used by Schmidt et al., the phase sensitivity is limited by the passive mechanical stability of the optical interferometer. Consequently, in order to reach high sensitivity, the sample should be chopped so that the signal is detected at frequencies, at which seismic and acoustic noise may be neglected. This might not be a problem in those cases, where an atomic or molecular beam must be used in order to avoid the Doppler effect. Then, chopping the sample simply can be realized by using a mechanical or optical chopper.

2 Theory of operation

In this section the theory of operation for the novel method is developed and the optimum conditions for operation are discussed.

An optical field described by $\mathcal{E}_{\mathrm{IN}} = \mathcal{E}_0 \exp(\mathrm{i}\omega t)$ enters the interferometer at the beam splitter M1, as shown in Fig. 2. The amplitude reflectivities of both beam splitters are denoted by r_1 and r_3, respectively. The beam splitters are assumed to be ideal: $r_i^2 + t_i^2 = 1$. The reflectivity of the mirrors is assumed to equal unity. $l_1 + l_\mathrm{a}$ gives the test arm physical length, l_2 denotes the distance between the input beam splitter M1 and the phase modulator (EOM), and l_b denotes the distance between the phase modulator and the output beam splitter. The photodiodes at the output of the interferometer are placed at distances L_1 and L_2 from M3, respectively. An optical field $\mathcal{E}$ interacting with the sample being placed within the test arm experiences some phase shift φ_m and absorption $(1 - t_\mathrm{m})$, so that one may write $\mathcal{E} \to \mathcal{E} \times t_\mathrm{m} \exp(\mathrm{i}\varphi_\mathrm{m})$. Finally, an optical field $\mathcal{E}$ passing the electro-optic phase modulator placed within the reference arm will undergo some phase modulation: $\mathcal{E} \to \mathcal{E} \times \exp(\mathrm{i}\, M_\mathrm{P} \sin \Omega t)$. As an example, we give the optical fields at the photodiode of output 1. The contributions from the test arm ($\mathcal{E}_\mathrm{T}$) and from the reference arm ($\mathcal{E}_\mathrm{R}$) are:

$$\begin{aligned} \mathcal{E}_\mathrm{T} &= \mathcal{E}_0\, r_1\, (-r_3)\, t_\mathrm{m}\, \mathrm{e}^{\mathrm{i}\,(\varphi_1+\varphi_\mathrm{a}+\psi_1+\varphi_\mathrm{m})}\,, \\ \mathcal{E}_\mathrm{R} &= \mathcal{E}_0\, t_1\, t_3\, \mathrm{e}^{\mathrm{i}\,(\varphi_2+\varphi_\mathrm{b}+\psi_1)}\, \mathrm{e}^{\mathrm{i}\, M_\mathrm{P} \sin(\phi_1)}\,. \end{aligned} \tag{3}$$

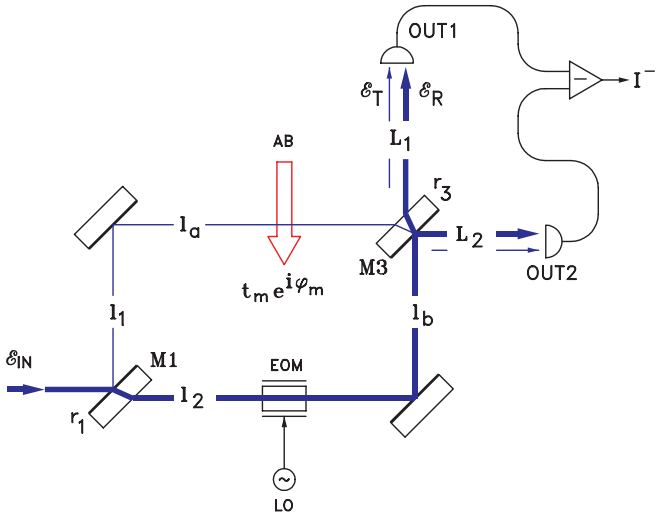

Fig. 2. Theory of operation of the novel spectroscopic method. The probe field $\mathcal{E}_{\rm IN}$ enters the interferometer at the strongly unbalanced beam splitter M1. An electro-optic phase modulator (EOM) is placed within the reference arm of the interferometer. A chopped atomic beam (AB) intersects the test arm. Both paths are recombined at the balanced beam splitter M3. The signal from both of the photodiodes at the outputs are subtracted to yield I^-. φ_i, ψ_i: optical phase shifts, r_i: amplitude reflectivity coefficients. For details see text

Here, $\varphi_i = l_i \times \omega/c$ for $i \in \{1, 2, a, b\}$ and $\psi_i = L_i \times \omega/c$ for $i \in \{1, 2\}$ mean optical phases, whereas $\phi_i = \Omega t + (l_{\rm b} + L_i) \times \Omega/c$ for $i \in \{1, 2\}$ describe microwave phases. The differential mode signal I^- derived from the two photodetectors can be written as $I^- := I_1 - g\, I_2$, where g accounts for a possible difference in the sensitivity of the detectors. Expanding the signal into Bessel functions of the first kind, $J_{\rm m} \equiv J_{\rm m}(M_{\rm P})$, we find:

$$
\begin{aligned}
I^- = I_0 \Big[& t_{\rm m}^2 \left[\tilde{r}^{\,2} - g\,\tilde{t}^{2}\right] + \left[(\tilde{r}\,\kappa)^2 - g\,(\tilde{t}\,\tilde{\kappa})^2\right] \\
& - 2t_{\rm m}\, \cos\left(\varphi_{\rm m} + \Delta\varphi_L\right) \left[\tilde{r}^{\,2}\kappa + g\,\tilde{t}^{2}\tilde{\kappa}\right]\, J_0 \\
& - 4t_{\rm m}\, \cos\left(\varphi_{\rm m} + \Delta\varphi_L\right) \\
& \times \sum_{n=1}^{\infty} J_{2n} \left\{ \tilde{r}^{\,2}\kappa\, \cos\left(2n\Phi_1\right) + g\,\tilde{t}^{2}\tilde{\kappa}\, \cos\left(2n\Phi_2\right) \right\} \\
& - 4t_{\rm m}\, \sin\left(\varphi_{\rm m} + \Delta\varphi_L\right) \\
& \times \sum_{n=0}^{\infty} J_{2n+1} \Big\{ \tilde{r}^{\,2}\kappa\, \sin\left[(2n+1)\Phi_1\right] \\
& \qquad + g\,\tilde{t}^{2}\tilde{\kappa}\, \sin\left[(2n+1)\Phi_2\right] \Big\} \Big] ,
\end{aligned}
\tag{4}
$$

where

$$
\Delta\varphi_L = (\varphi_1 + \varphi_{\rm a}) - (\varphi_2 + \varphi_{\rm b}) \tag{5}
$$

is the optical phase difference between the arms of the empty interferometer, and $\tilde{r} = r_1\, r_3$ and $\tilde{t} = r_1\, t_3$ describe the amplitude transmission coefficients for the transfer of the probe field from the input to outputs 1 and 2 via the test arm, respectively. Similarly, $\tilde{r}\kappa = t_1\, t_3$ and $\tilde{t}\tilde{\kappa} = t_1\, r_3$ give the amplitude transmission coefficients for a transfer of the probe field from the input to outputs 1 and 2 via the reference arm, respectively. Finally, I_0 means the optical power injected into the interferometer. As a first result, we conclude from the equation above, that the demodulation of the signal at the modulation frequency and at its harmonics provides a signal to lock the interferometer at a "dark fringe" ($\sin\left[\Delta\varphi_L + \varphi_{\rm m}\right] = 0$) or at a "half fringe" ($\cos\left[\Delta\varphi_L + \varphi_{\rm m}\right] = 0$).

In order to simplify the expression, we first discuss the physical meaning of the microwave phases ϕ_1 and ϕ_2. The corresponding terms within the sum over the Bessel functions have the form

$$
\begin{aligned}
a \sin\left(m\Omega t\right) + b \sin\left(m\Omega t + \left[L_2 - L_1\right]\Omega/c\right) \\
= d \sin\left(m\Omega t + \psi'\right)
\end{aligned}
$$

for certain d and ψ' depending on a, b, and $\left[L_2 - L_1\right]\Omega/c$. It can be shown, that a variation of $L_2 - L_1$ will change ψ' and hence introduce a phase shift of the modulation signal with respect to the phase of the local oscillator. In addition, the amplitude d of the signal will vary sinusoidally with $L_2 - L_1$ and may even vanish for certain parameters. Therefore, both of the "signal paths" which are formed by the output beam splitter, by each of the photodetectors and by the subtracter, may be interpreted in terms of a microwave interferometer (see Fig. 2). However, there is no square-law detector following the "output beam splitter" (the subtracter), so there is no complete analogy to a standard interferometer. Nevertheless, we may conclude two important results from this discussion. First, differential mode variations of the photodetector positions will change the phase and amplitude of the signal at the modulation frequency and its harmonics and therefore will only introduce *relative* noise to the signal. This means, that any variation of $L_2 - L_1$ will not affect the "locking points" $\sin\left(\varphi_{\rm m} + \Delta\varphi_L\right) = 0$ and $\cos\left(\varphi_{\rm m} + \Delta\varphi_L\right) = 0$ of the interferometer. Second, we notice that for modulation frequencies in the MHz regime the phase difference $\phi_2 - \phi_1 = (L_2 - L_1)\Omega/c$ can usually be kept small and variations of $L_2 - L_1$ due to seismic and acoustic interference will give rise to relative signal noise in the ppm to ppb range only. For sake of simplicity, we therefore will assume $\phi_2 = \phi_1 = \Omega t$ in the following.

We continue the discussion by asking for the optimum choice of the beam splitter reflectivities. From (4) it follows, that maximum signal at the modulation frequency and its harmonics is achieved, if

$$
I_0\, J_{\rm m}(M_{\rm P}) \left[\tilde{r}^{\,2}\kappa + g\tilde{t}^{2}\tilde{\kappa}\right] = I_0\, J_{\rm m}(M_{\rm P})\, 2 r_1\, r_3 \sqrt{1 - r_1^2}\, \sqrt{1 - r_3^2} \tag{6}
$$

becomes maximum, where balanced photodetectors ($g \equiv 1$) have been assumed. Usually, the experimental situation implies some convenient test field power $I_{\rm IZ}$ in the interaction zone, which defines the input beam splitter reflectivity for a given probe laser power I_0: $r_1^2 = I_{\rm IZ}/I_0$. Expression (6) will be maximum for a balanced beam splitter at the output of the interferometer, $r_3^2 = 1/2$. Using these reflectivities, the signal "strength" (6) may be rewritten as

$$
I_0\, J_{\rm m}(M_{\rm P}) \left[\tilde{r}^{\,2}\kappa + g\tilde{t}^{2}\tilde{\kappa}\right] \approx \sqrt{I_{\rm IZ}} \times \sqrt{J_{\rm m}^2(M_{\rm P})\, I_0} \tag{7}
$$

in the limit of $I_{\rm IZ} \ll I_0$. As in FMS, this clearly demonstrates that the signal arises from the beat of the optical field of the

test arm and certain phase modulation sidebands of the reference arm. Hence, in order to achieve a good signal-to-noise ratio, a strong probe $I_0 \gg I_{IZ}$, an unbalanced input beam splitter $r_1^2 \ll 1$ and a balanced output beam splitter $r_3^2 = 1/2$ have to be used.

In a real experiment the output beam splitter ($r_3^2 = 1/2 + \delta R$) and the photodetectors ($g = 1 + \delta g$) are never exactly balanced but their unbalance can be kept small ($|\delta g|, |\delta R| \ll 1$). Although it is not essential, we will further assume for sake of simplicity, that the absorption-induced loss introduced to the test field is small. Consequently, $t_m = \exp(-\alpha_m/2) \approx 1 - \alpha_m/2$, where α_m describes the relative absorption of the test field power. Further, for small phase shifts $\varphi_m \ll 1$, sine and cosine expressions of (4) can be expanded with respect to this quantity. Then, two modes of operation may be distinguished, which will be discussed in the following: operation at a "dark fringe", $\sin \Delta\varphi_L = 0$, and operation at a "half fringe", $\cos \Delta\varphi_L = 0$. Please note that for unbalanced beam splitters the "dark port" will not really be dark.

For operation at a "dark fringe" we find the following contributions to the signal at dc, at the modulation frequency Ω and at its second harmonic 2Ω:

$$\begin{aligned} I_{DC}^- &\approx -I_0 \times \left[2 J_0(M_P)\, r_1\, t_1 \left(1 - \frac{\alpha}{2} + \frac{\delta g}{2}\right) \right. \\ &\qquad \left. + \frac{1}{2}\delta g - 4\left(r_1^2 - \frac{1}{2}\right)\delta R \right], \\ I_{\Omega}^- &\approx -4 I_0 \times J_1(M_P)\, r_1\, t_1\, \varphi_m \times \sin \Omega t\,, \\ I_{2\Omega}^- &\approx -4 I_0 \times J_2(M_P)\, r_1\, t_1 \left(1 - \frac{1}{2}\alpha + \frac{1}{2}\delta g\right) \times \cos 2\Omega t\,. \end{aligned} \tag{8}$$

Based on the assumptions introduced above, the signal has been expanded with respect to α_m, φ_m, δg, and δR where second and higher order terms have been neglected. As can be seen, the term oscillating at the modulation frequency provides information about the phase shift φ_m of the optical test field, whereas deviations from perfect balance of the beam splitter and of the photodetectors do not contribute to first order [19]. Both, the dc signal and the contribution at $2\,\Omega$ provide the information about the absorption, which may be offset by the unbalance of the output beam splitter and of the photodetectors. Utilizing the contribution at the second harmonic offers some advantages since the signal is less affected by unbalance and by $1/f$ electronic noise than the dc contribution. However, this requires additional HF electronics.

For the second mode of operation, for operation at a "half fringe", we similarly find the following expressions for the contributions to the signal:

$$\begin{aligned} I_{DC}^- &\approx I_0 \times \left[2 r_1\, t_1\, J_0(M_P)\, \varphi_m - \frac{1}{2}\delta g + 4\left(r_1^2 - \frac{1}{2}\right)\delta R \right], \\ I_{\Omega}^- &\approx -4 I_0 \times J_1(M_P) r_1\, t_1 \left(1 - \frac{1}{2}\alpha + \frac{1}{2}\delta g\right) \times \sin \Omega t\,, \\ I_{2\Omega}^- &\approx 4 I_0 \times J_2(M_P) r_1\, t_1 \varphi_m \times \cos 2\Omega t\,. \end{aligned} \tag{9}$$

As far as the dc part of the signal is concerned, this mode of operation is comparable to the setup used by Schmidt et al. [16]. From the equation above it is clear, that especially for a strongly unbalanced *input* beam splitter an imbalance of the output beam splitter will introduce a large offset to the signal. For this reason, it is much more convenient to extract the phase shift information from the signal at the second harmonic of the modulation frequency, while the loss now can be determined from the contribution at the modulation frequency itself.

Comparing the two modes of operation, we find that they both provide the information about the optical phase shift without offsets, if detected properly. Further, the transmitted amplitude of the test field is measured rather than the absorbed. Please also note, that for both operational modes there is no cross-talking between the phase and the absorption signal to first order. If the interferometer is operated as an active null instrument for phase shift detection so that $\sin(\Delta\varphi_L + \varphi_m) = 0$ or $\cos(\Delta\varphi_L + \varphi_m) = 0$ for operation at a "dark fringe" or at a "half fringe", respectively, cross-talking is avoided even for large phase shifts and for large absorption, as can be seen from (4). Additionally, imbalance of the output beam splitter or of the photodetectors do not introduce any offsets to the phase shift measurement, if the phase shift information is not obtained from the dc contribution to the signal. Hence, the interferometer may be locked exactly at the operating point as desired, which is essential for avoiding cross-talking effects. Finally, only operation at a "dark fringe" allows us to use a single HF demodulation scheme, so that this operational mode appears to be the most simple one.

3 Signal-to-noise analysis

In this section an analysis of the most important technical noise sources and a discussion of the signal-to-noise ratio is presented. This analysis provides useful information about the optimum phase modulation index and the geometry of the interferometer.

The most important sources for signal noise are laser power noise, laser frequency noise, and mechanical noise of the interferometer which is introduced by seismic and acoustic noise of the environment. We will only give a rough estimation about shot noise, since the sensitivity of the present setup is well above this fundamental limit.

In an experiment, the laser power I_0 will be affected by noise. Hence, one may write $I_0 = \hat{I}_0\,(1 + i(t))$, where $i(t)$ is the relative power noise (RIN) of the laser and $\hat{I}_0$ denotes the mean power averaged over a certain measurement interval T. Defining the Fourier transform of $i(t)$ by $\hat{i}_T(f) = \int_{-T/2}^{T/2} i(t) \exp(i 2\pi f t)\, dt$, the single-sided power spectral density of the relative intensity noise is given by [20]

$$S_P\{i(t)\}(f) = \lim_{T\to\infty} \frac{2}{T}\ \hat{i}_T(f) \times \hat{i}_T^*(f)\,. \tag{10}$$

The signal noise arising from RIN then is given by

$$\begin{aligned} \delta I^-(t) = \hat{I}_0(t)\ \times\ i(t) \Bigg\{ A_{DC} + \sum_{n=1}^{\infty} C_{2n}\ \cos[2n\, 2\pi f_m t] \\ + \sum_{n=0}^{\infty} C_{2n+1}\ \sin[(2n+1)\, 2\pi f_m t] \Bigg\}, \end{aligned} \tag{11}$$

where A_{DC} and C_n are defined according to (4) and $f_{\mathrm{m}} = \Omega/(2\pi)$ is the modulation frequency. Now, the Fourier transform $\widehat{\delta I^-}_{\mathrm{T}}(f)$ of $\delta I^-(t)$ has to be calculated. Next, in analogy to (10), the power spectral density of the signal noise due to RIN may be obtained from the Fourier transform. We find:

$$S_{\mathrm{p}}\left\{\delta I^-(t)\right\}(f) \approx \hat{I}_0^2 \times \left\{ |A_{\mathrm{DC}}|^2 \, S_{\mathrm{p}}\left\{i(t)\right\}(f) + \frac{1}{4}\sum_{n=1}^{\infty} |C_n|^2 \left\{ S_{\mathrm{p}}\left\{i(t)\right\}(|n f_{\mathrm{m}} - f|) + S_{\mathrm{p}}\left\{i(t)\right\}(n f_{\mathrm{m}} + f) \right\} \right\}. \tag{12}$$

It has been assumed that the RIN from different Fourier components is not correlated, so that on the r.h.s. of (10) all terms except those taken at identical frequency cancel. From the power spectral density the rms noise signal for a given integration time, i.e. for a certain detection bandwidth Δf, can be calculated:

$$I^-_{\mathrm{rms,\,min}} := \sqrt{\Delta f} \times \sqrt{S_{\mathrm{p}}\left\{\delta I^-(t)\right\}}. \tag{13}$$

This rms noise signal reveals the rms signal, which can be recorded with unity signal-to-noise ratio. Hence, it determines the minimum detectable phase shift and loss signal and thus defines the sensitivity limit. Combining (8), (9) and (13), the sensitivity for phase shift and loss detection can be calculated. For operation at a "dark fringe" (8), we find

$$\alpha_{\mathrm{rms,\,min,\,DC}} = 2 \times \sqrt{S_{\mathrm{p}}\left\{i(t)\right\}(0) + 2\left(\frac{J_2}{J_0}\right)^2 S_{\mathrm{p}}\left\{i(t)\right\}(2 f_{\mathrm{m}})} \times \sqrt{\Delta f}, \tag{14}$$

$$\varphi_{\mathrm{rms,\,min,\,}f_{\mathrm{m}}} = \sqrt{1 + \left(\frac{J_0}{J_1}\right)^2} \times \sqrt{S_{\mathrm{p}}\left\{i(t)\right\}(f_{\mathrm{m}})} \times \sqrt{\Delta f}, \tag{15}$$

$$\alpha_{\mathrm{rms,\,min,}\,2f_{\mathrm{m}}} = \sqrt{S_{\mathrm{p}}\left\{i(t)\right\}(0) + \frac{J_0^2 + J_4^2}{J_2^2} S_{\mathrm{p}}\left\{i(t)\right\}(2 f_{\mathrm{m}})} \times \sqrt{\Delta f}. \tag{16}$$

Since RIN will decrease at high frequencies, only noise contributions from RIN at dc, f_{m}, and $2 f_{\mathrm{m}}$ are considered. Please note, that at dc the minimum detectable loss is twice as large as expected for a direct loss detection. This is due to the fact, that the method described here measures the damping of the test field amplitude rather than the damping of the test field power. For operation at a "half fringe" the calculation yields

$$\varphi_{\mathrm{rms,\,min,\,DC}} = \sqrt{2} \times \left|\frac{J_1}{J_0}\right| \times \sqrt{S_{\mathrm{p}}\left\{i(t)\right\}(f_{\mathrm{m}})} \times \sqrt{\Delta f}, \tag{17}$$

$$\alpha_{\mathrm{rms,\,min,\,}f_{\mathrm{m}}} = \sqrt{S_{\mathrm{p}}\left\{i(t)\right\}(0) + \left(1 + \frac{J_3^2}{J_1^2}\right) S_{\mathrm{p}}\left\{i(t)\right\}(2 f_{\mathrm{m}})} \times \sqrt{\Delta f}, \tag{18}$$

$$\varphi_{\mathrm{rms,\,min,}\,2f_{\mathrm{m}}} = \frac{1}{2} \times \sqrt{\frac{J_1^2 + J_3^2}{J_2^2}} \times \sqrt{S_{\mathrm{p}}\left\{i(t)\right\}(f_{\mathrm{m}})} \times \sqrt{\Delta f}, \tag{19}$$

where again high-frequency RIN ($f > 2 f_{\mathrm{m}}$) has been neglected. From (15), (17), and (19) it follows that shot-noise-limited phase-shift detection is achievable if the modulation frequency is large enough, so that RIN at f_{m} and its harmonics may be neglected when compared to shot noise. However, as can be seen from (14), (16), and (18), the loss detection always contains RIN from dc, where shot-noise-limited power stability usually can not be achieved for technical reasons.

The noise analysis clearly shows that the optimum modulation index depends on the spectral properties of the RIN. The laser system [21] used for the experimental investigations on the novel spectroscopic method exhibits a roughly white RIN for Fourier frequencies up to 3 MHz. This is about twice the modulation frequency ($f_{\mathrm{m}} = 1.8$ MHz) that has been applied, so that as a good approximation $S_{\mathrm{p}}\left\{i(t)\right\}(0) = S_{\mathrm{p}}\left\{i(t)\right\}(f_{\mathrm{m}}) = S_{\mathrm{p}}\left\{i(t)\right\}(2 f_{\mathrm{m}})$ may be assumed. Based on this simplification, the optimum choice for the phase modulation index can be evaluated. This is shown for both modes of operation, that is for operation at a "dark fringe" in Fig. 3a and for operation at a "half fringe" in Fig. 3b. In these figures the minimum detectable loss $\alpha_{\mathrm{rms,\,min}}$ and phase shift $\varphi_{\mathrm{rms,\,min}}$ normalized to $\sqrt{S_{\mathrm{p}}\left\{i(t)\right\} \times \Delta f}$ are given for detection at dc, at f_{m} and at $2 f_{\mathrm{m}}$.

For operation at a "dark fringe" (Fig. 3a), the optimum phase modulation index is $M_{\mathrm{P}} \approx 2.3$, if phase shift and loss

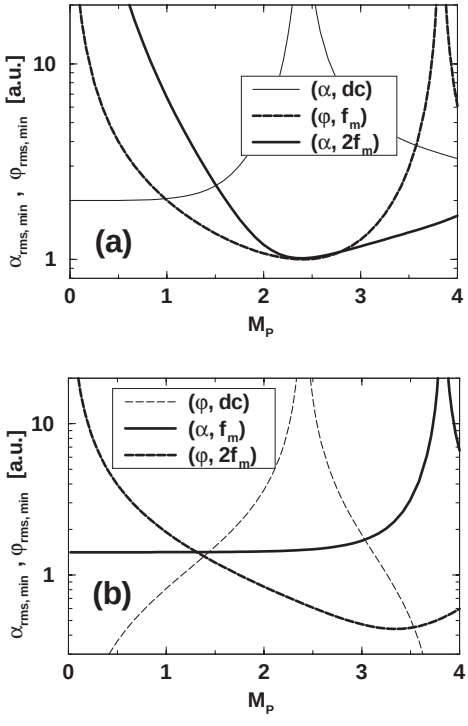

Fig. 3a,b. Optimum phase-modulation index for operation at a "dark fringe" (**a**) and at a "half fringe" (**b**). Minimum detectable loss and phase shift are shown vs. phase modulation index M_{P}. Loss and phase shift are normalized to $\sqrt{S_{\mathrm{p}}\left\{i(t)\right\}(0) \times \Delta f}$. Loss and phase-shift detection are shown in *solid* and *dashed lines*, respectively. Detection at dc and ac are given in *thin* and *thick lines*, respectively

are detected at ac. However, the most simple way of operation from the electronics point of view is achieved with loss detection at dc. Then, the optimum phase modulation index is $M_\mathrm{p} \approx 1.5$. This setup was chosen for the experiment. For a much larger modulation index, the loss sensitivity is strongly reduced or even vanishes at $M_\mathrm{P} = 2.4$. At this modulation depth, the carrier field within the reference arm is suppressed, as follows from the zero of the Bessel function J_0.

For operation at a "half fringe" (Fig. 3b), optimum phase shift and loss sensitivity are achieved at different phase modulation indices. As a compromise, a modulation index of $M_\mathrm{P} \approx 3$ is adequate, where the phase shift sensitivity overcomes the sensitivity for operation at a "dark fringe" by a factor of 2 and the loss sensitivity is worse by a factor of $\sqrt{2}$.

Finally it should be emphasized that for the laser system and the modulation frequency used here, the minimum detectable relative loss and phase shift will be limited by the RIN at dc and roughly be given by its magnitude. If lasers were used featuring shot-noise-limited power stability at the modulation frequency or if the modulation frequency was sufficiently increased, then shot-noise-limited phase-shift detection would be achievable.

A measurement of the optical phase shift always yields $\varphi = \Delta\varphi_L + \varphi_\mathrm{m}$. Hence, it can not be decided whether the phase shift is introduced by the medium or by a variation of $\Delta\varphi_L$. According to (5), phase-shift noise will be introduced by residual laser-frequency noise and by mechanical noise of the interferometer. As for the analysis of laser-power noise, this rms phase shift error measured within the detection bandwidth Δf will define the minimum phase shift due to the medium, which can be detected with unity signal-to-noise ratio. From (5) it follows, that this sensitivity limit is given by

$$\varphi^2_{\mathrm{rms,\,min}} = \left\{ \left(\frac{\Delta L_0}{c}\right)^2 \times S_\mathrm{p}\{\delta\omega(t)\}(f) + \left(\frac{\omega_0}{c}\right)^2 \times S_\mathrm{p}\{\delta(\Delta L)(t)\}(f) \right\} \times \Delta f\,, \qquad (20)$$

where $\Delta L_0 + \delta(\Delta L)(t) = [(l_1 + l_\mathrm{a}) - (l_2 + l_\mathrm{b})](t)$ according to Fig. 2 and $\omega(t) = \omega_0 + \delta\omega(t)$ denotes the instantaneous laser frequency. From the equation above it follows, that noise contribution from laser-frequency noise can be suppressed, if a white-light interferometer ($\Delta L_0 = 0$) is used, a condition well known from interferometry. The second term of (20) introduces noise arising from differential mode geometry fluctuations of the interferometer. For a Mach–Zehnder interferometer, this contribution can be kept small even for low Fourier frequencies, since for proper mechanical construction differential mode drifts can be avoided to some extent. Nevertheless, the phase-shift sensitivity will always be limited by the passive stability of the interferometer. Therefore, good seismic and acoustic isolation of the setup from the environment is essential. In general, high sensitivity will only be accessible if phase shift (and loss) detection is shifted from dc to higher frequencies (kHz), where seismic and acoustic interference can reduced by passive isolation, so that it can be neglected when compared to laser noise. For example, this can be realized by chopping the sample which is an atomic beam in our case.

Finally we will give a rough estimation about the significance of quantum noise, as far as is related to the optical fields (shot noise). A rigorous shot-noise analysis requires a quantum mechanical treatment of the interferometer, of the electro-optic phase modulator and of the balanced detector. To our knowledge, a shot-noise analysis of a compound system like the one discussed here has not been done so far. For example, Caves [22] has presented a shot-noise analysis that may be applied to Mach–Zehnder interferometers. However, this analysis is based on the condition that none of the fields is modulated and that both of the beam splitters are balanced. Hence, it does not meet our requirements. The latter argument also applies to the discussion about non-stationary shot noise given by Niebauer et al. [23]. Further, these authors did not consider balanced detection of the signal, so that their discussion as well does not match our situation. Therefore, we will simply assume that the order of magnitude of signal shot noise is given by the shot noise of the weak test field, if it was directly detected with an ideal photodetector. This assumption seems reasonable as can be seen from the discussion of shot noise in homodyne and heterodyne detection [24]. The RIN due to shot noise of the weak test field is determined by [20]

$$S_\mathrm{p}\{i(t)\}(f) = 2\frac{h\nu}{r_1^2\,P_0}\,, \qquad (21)$$

where P_0 is the laser power at the input beam splitter. The factor of 2 enters from the fact that $S_\mathrm{p}\{i(t)\}(f)$ is a single-sided power spectral density. In our experiments, the power in the interaction volume is about $r_1^2\,P_0 \sim 20\,\mu\mathrm{W}$. At a wavelength of $\lambda = 423\,\mathrm{nm}$ this results in a RIN of $S_\mathrm{p}^{1/2}\{i(t)\}(f) \approx 2\times10^{-7}/\sqrt{\mathrm{Hz}}$, which is less than our current (technical) RIN at the corresponding Fourier frequencies by a factor of about 50. Hence, we conclude that our sensitivity is not yet shot-noise-limited.

4 Experimental realization

Finally, a description of the experimental setup and an experimental determination of the sensitivity achieved so far are given. To demonstrate the potential of the novel method, the spectroscopic investigation of the Ca-resonance transition $4s^2\ {}^1S_0 \rightarrow 4s4p\ {}^1P_1$ at 423 nm is presented.

The interferometer is operated completely in an UHV ($< 10^{-7}$ mbar) environment. The vacuum chamber is mechanically decoupled from the interferometer, which is connected to the optical table by an intra-vacuum 2-stage mount. This consists of three legs, carrying an intermediate mass (≈ 35 kg), which is mechanically decoupled from the legs via a number of self-made rubber cylinders qualified for UHV operation. The interferometer itself (≈ 30 kg) is placed upon the intermediate mass with a set of rubber cylinders between them. The components of the interferometer are interconnected by three rods made of Zerodur in order to reduce thermal drifts of the apparatus. The vacuum chamber also includes a Ca oven used to produce an atomic beam, which can be chopped mechanically at frequencies up to 4 kHz, where $f_\mathrm{C} = 1.77\,\mathrm{kHz}$ is the value usually chosen.

We use an intra-vacuum polarizer (extinction $> 10^{-7}$ nominal) before the input beam splitter of the interferometer. The optical beam traverses the input beam splitter at an

angle that is close to the Brewster angle. This way, an uncoated substrate provides the realization of highly unbalanced tunable input beam splitters. So far, an effective splitting of 1 : 7 has been employed, where the loss due to the phase modulator has been taken into account. The laser power within the test arm usually is taken to be $r_1^2 P_0 \approx 20\,\mu\mathrm{W}$, whereas the power of the reference field at the output beam splitter is about $P_0 \approx 140\,\mu\mathrm{W}$. The EOM is driven at a frequency of $f_\mathrm{m} = 1.8\,\mathrm{MHz}$ with a phase modulation index of $M \approx 1$.

The interferometer is operated as an active null instrument. Therefore, we lock the interferometer to a "dark fringe". The error-signal is derived from the balanced interferometer output and is demodulated at f_m. After some filtering and amplification, the signal is applied to a piezo-electric-transducer (PZT, Fig. 1) in order to compensate for low-frequency phase noise and drifts. The high-frequency part of the signal is applied to the EOM. This way we achieve a locking bandwidth (unity gain) of 50 kHz with the cross-over between PZT- and EOM loop at Fourier frequencies below $f = 200\,\mathrm{Hz}$ and a $-12\,\mathrm{dB/oct.}$ suppression of PZT gain against EOM gain. We have ensured that the gain of the EOM loop exceeds 40 dB (50 dB typically) within the frequency band of 200 Hz to 2 kHz. To extract the optical phase shift of the test field due to the interaction with the atoms, the feedback signal for the EOM is probed with a high-impedance probe, filtered by an 8th-order bandpass and then detected with a dual-phase lock-in amplifier. By detecting the servo-signal for the EOM, calibration of the phase shift signal is most simple since the half-wave voltage of the EOM is known. Further, this calibration does not depend on experimental conditions, for example on the probe field power. For the sake of experimental simplicity, the absorption signal is derived from the dc part of the balanced interferometer output and not from the signal at $2 f_\mathrm{m}$. After some amplification and filtering with an 8th-order bandpass, the loss signal is detected with a dual-phase lock-in amplifier as well.

For an experimental determination of the current phase shift sensitivity, the setup was operated as described above but with the phase-shift lock-in amplifier replaced by a spectrum analyzer. The oven was not heated but the atomic beam chopper was driven at $f = 146\,\mathrm{Hz}$ which would result in a chopping frequency of $f_\mathrm{C} = 1752\,\mathrm{Hz}$. The laser was free-running for this measurement. The power spectral density of the phase noise is shown in Fig. 4. A number of resonances can be identified, which are due to interference of mechanical noise arising from the turbo-pumps ($a_n = n \times 750\,\mathrm{Hz}$) and from the atomic beam chopper ($b_n = n \times 146\,\mathrm{Hz}$). The background noise is almost white and is close to $S_\mathrm{P}^{1/2}\{\varphi_\mathrm{m}(t)\}(f) \approx 1.1 \times 10^{-5}\,\mathrm{rad}/\sqrt{\mathrm{Hz}}$, determining the current phase-shift sensitivity. At frequencies above $f \approx 1.2\,\mathrm{kHz}$, the noise at the harmonics of the mechanical rotation frequency of the atomic beam chopper is negligible. Therefore, a chopping frequency of about $f_\mathrm{C} \approx 1770\,\mathrm{Hz}$ usually is chosen.

We next discuss the current limitations for the phase-shift sensitivity. Following [21, 25], the high-frequency RIN of the laser is close to $S_\mathrm{P}^{1/2}\{i(t)\}(1.8\,\mathrm{MHz}) = 5.0 \times 10^{-6}/\sqrt{\mathrm{Hz}}$. According to (15), this will give rise to a phase noise of $S_\mathrm{P}^{1/2}\{\varphi_\mathrm{m}(t)\}$ $(1.7\,\mathrm{kHz}) \approx 6.5 \times 10^{-6}\,\mathrm{rad}/\sqrt{\mathrm{Hz}}$ for a phase modulation index of $M = 1.57$. This is 4.6 dB less than the sensitivity limit achieved experimentally. The power spectral density of the frequency noise of the free-running laser

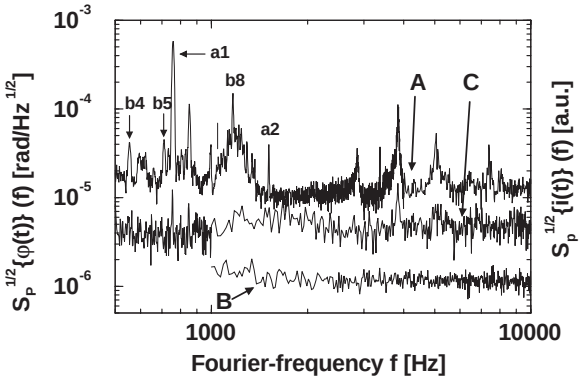

Fig. 4. Sensitivity for phase-shift detection. The square root of the power spectral density of the phase-shift noise is shown. (A) phase noise of the interferometer measured with a free-running laser. The phase modulation index is $M = 1.57$. (B) detector electronic noise. Phase noise resulting from high-frequency RIN and from laser-frequency noise is $\approx 6.5 \times 10^{-6}\,\mathrm{rad}/\sqrt{\mathrm{Hz}}$ and $\approx 1.2 \times 10^{-5}\,\mathrm{rad}/\sqrt{\mathrm{Hz}}$ at $f \approx 1.7\,\mathrm{kHz}$, respectively. (C) low-frequency RIN [a.u.], which does not limit the phase-noise sensitivity but which is shown here for the discussion of the structure of the noise spectra. The nth harmonic resonances a_n and b_n result from mechanical interference of the turbo-pumps and of the atomic beam chopper, respectively

exceeds $S_\mathrm{P}^{1/2}\{\delta\omega(t)\}(f) = 7.5\,\mathrm{kHz}/\sqrt{\mathrm{Hz}}$ at $f = 1.7\,\mathrm{kHz}$ and can be estimated to be close to $28\,\mathrm{kHz}/\sqrt{\mathrm{Hz}}$ [21, 25]. Following (20) this introduces a phase noise of $S_\mathrm{P}^{1/2}\{\varphi_\mathrm{m}(t)\}(1.7\,\mathrm{kHz})$ $\approx 1.2 \times 10^{-5}\,\mathrm{rad}/\sqrt{\mathrm{Hz}}$ for an interferometric arm length difference of $\Delta L_0 = 13\,\mathrm{cm}$. Since the background noise is almost white we may assume, that acoustic and seismic noise directly interfering with the interferometer do not contribute to it significantly. Provided RIN and laser-frequency noise are uncorrelated (which strictly speaking will not be the case), both noise sources would add up to a phase-shift sensitivity of $S_\mathrm{P}^{1/2}\{\varphi_\mathrm{m}(t)\}$ $(1.7\,\mathrm{kHz}) = 1.4 \times 10^{-5}\,\mathrm{rad}/\sqrt{\mathrm{Hz}}$, which is 1.9 dB more than the sensitivity limit determined experimentally. This small discrepancy can be attributed to the uncertainty in knowledge of the laser frequency noise and the EOM half-wave voltage. Hence, we conclude that for the measurement presented here, the phase-shift sensitivity is limited by residual laser-frequency noise.

To underpin this conclusion, the low-frequency RIN is shown as curve C in Fig. 4. From Sect. 3 we know, that RIN at low Fourier frequencies does not contribute to the phase-shift signal noise. Nevertheless, it can be seen that the phase noise spectrum shows the same resonances as does the RIN spectrum at Fourier frequencies above 3.5 kHz. This can be explained as follows: The optical power is provided by a single resonant external cavity frequency-doubling unit, which is stabilized in frequency to a free-running diode laser system. The unity gain frequency of the corresponding servo-loop is about 6 kHz, so that at Fourier frequencies well below 6 kHz the cavity can "follow" the frequency excursions of the diode laser. Therefore, resonances of the frequency noise spectrum at Fourier frequencies up to a few kHz do not appear within the power noise spectrum of the laser. However, at Fourier frequencies comparable with or greater than $\approx 6\,\mathrm{kHz}$, these frequency-noise resonances will be recovered within the power noise spectrum. In conclusion this explains why the resonances within the phase noise spectrum coincide with the *low-frequency* resonances of the power noise spectrum at Fourier frequencies above a few kHz, and why they do not at

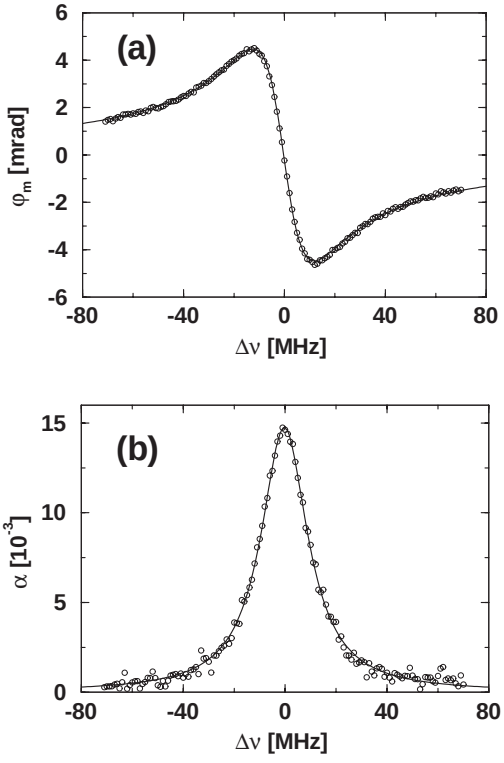

Fig. 5a,b. Ca resonance transition $4s^2\ ^1S_0 \rightarrow 4s4p\ ^1P_1$, $\Delta m = 0$. **a** shows the optical phase shift, **b** shows the natural logarithm of the relative transmission $\alpha_0 \times L_{IZ}$, where α_0 is the absorption coefficient and L_{IZ} gives the interaction length. An atomic beam is used for the measurement. Interaction length: $l_{\text{eff}} \approx 1$ mm. Atomic density: $N \approx 4 \times 10^8$ cm^{-3}. Integration time: 1 s. Zero frequency detuning corresponds to the nominal resonance frequency. The *solid lines* depict a fit of a theoretical two-level spectrum. The fitted parameters are given within the text

frequencies below. We also conclude that it is consistent to attribute the peaks and the white background of the phase noise spectrum to laser-frequency noise.

As a demonstration of the potential provided by the novel method, we finally present the results of a spectroscopic investigation of the Ca resonance transition $4s^2\ ^1S_0 \rightarrow 4s4p\ ^1P_1$, $\Delta m = 0$, at 423 nm. For this experiment two lasers based on external-cavity SHG (second-harmonic generation) are used, the first of which is locked to the transition. This servo-loop utilizes a FMS setup based on a Ca heatpipe. A fraction of the first laser's fundamental power is shifted in frequency by 200 MHz and then is used as an optical local oscillator for phase locking of the second laser system. Applying a tunable microwave oscillator and a mixer, the second laser can be tuned in frequency with respect to the first laser. This second laser is used for measuring the optical spectra. The result of this experiment is shown in Fig. 5, where the optical phase shift and the negative natural logarithm of the transmission ($\alpha = \alpha_0 L_{IZ}$) are given. For this measurement the power in the test arm of the interferometer was 20 μW corresponding to an intensity of 0.4 mW/mm^2, which is about 1/3 of the saturation intensity [27]. The integration time was 1 s. The solid lines in Fig. 5 correspond to the theoretical spectrum of a two-level atom [4] fitted to the experimental data. For an interaction length of $L_{IZ} = 1$ mm the following parameters are obtained: $N = 4.1900(89) \times 10^8$ cm^{-3}, $\gamma/(2\pi) = 24.252(85)$ MHz, and $\Delta\nu = 3\,27(\,26)$ kHz from the phase shift data and $N = 3.451(23) \times 10^8$ cm^{-3}, $\gamma/(2\pi) = 22.41(21)$ MHz, and $\Delta\nu = 326(75)$ kHz from the absorption data. For these parameters, only statistical errors (one standard deviation) are given. Here, $\gamma/(2\pi)$ denotes the FWHM-linewidth and $\Delta\nu$ gives the detuning of the line center from the frequency expected. A non-zero detuning is obtained, if the laser field does not intersect the atomic beam at a right angle so that a Doppler shift can be observed.

The remarkable agreement between the fit parameters derived independently from the absorption and phase-shift measurement ($\Delta N/N = 0.18$, $\Delta\gamma/\gamma = 0.076$) should be pointed out. Nevertheless, the differences exceed the statistical errors given above. The difference between the atomic densities is attributed to inaccurate calibration of phase shift and absorption data. A calibration error enters into the phase-shift detection, if the EOM half-wave voltage is not precisely known (8%). For the calibration of the absorption data we estimate a slightly larger uncertainty, as a number of parameters and their experimental uncertainties enter (15%). We estimate the phase-modulation index to be the parameter introducing the largest uncertainty to the absorption calibration and the absorption calibration to be less accurate than the phase-shift calibration. We attribute the origin of the difference between the fitted linewidth data to technical problems in maintaining a constant phase modulation index during a single scan. Work is in progress to resolve this problem.

Although the origin of some systematic effects has not yet been fully resolved, the correspondence between theoretical and experimental data clearly demonstrates, that this novel method provides good signal-to-noise ratio even at low optical powers within the interaction zone. It also proves that cross-talking between the phase shift and absorption signal is avoided. Therefore, this method is well suited especially for those applications of precision spectroscopy, where accurate knowledge of absorption and index of refraction *profiles* is of major interest.

5 Conclusion

In this paper we have presented a novel spectroscopic method which is based on a phase-modulated interferometer. We have shown that this novel setup is well suited especially for experiments on novel optical media for which the simultaneous and high-precision measurement of absorption and index of refraction *profiles* is most important.

A comparison with competing methods of interferometry and FMS has revealed that only the novel method can simultaneously fulfill the essential requirements related to the study of novel optical media. In principle, shot-noise-limited sensitivity can be achieved for optical phase-shift detection (index of refraction measurement). Optical reference fields bypass the interaction zone avoiding a modification of the medium by the reference fields and vice versa. Cross-talking between the absorption and the index of refraction signal is avoided and a linear response is ensured even for large phase shifts ($\approx \pi$), provided that the interferometer is operated as an active null instrument. Implementing a strongly unbalanced input beam splitter, a strong reference field (optical LO) can be used to achieve a good signal-to-noise ratio even at low probe powers in the sample volume.

The theory of operation for the phase-modulated interferometer has been presented. Following this analysis we found that the absorption and the index of refraction (optical phase shift) can both be extracted from the differential mode output of the interferometer by demodulating the signal at the modulation frequency and its harmonics. Two useful modes of operation can be distinguished if the interferometer is operated as an active null instrument, that is operation at a "dark fringe" and operation at a "half fringe". A classical signal-to-noise analysis lead to an optimization of the phase-modulation index for both modes of operation. This signal-to-noise analysis has taken into account the most important sources of signal noise, that is laser power and laser frequency noise. The phase-shift sensitivity determined experimentally ($1.1 \times 10^{-5}\,\mathrm{rad}/\sqrt{\mathrm{Hz}}$ at a probe power of $\approx 20\,\mu\mathrm{W}$) was found to be in good agreement with the value calculated: it has been pointed out, that although laser-frequency noise is currently limiting the phase-shift sensitivity, shot-noise-limited sensitivity should be achievable experimentally. Further, it has been shown that absorption sensitivity will always be limited by low-frequency ("dc") laser-power noise ($2 \times 10^{-5}/\sqrt{\mathrm{Hz}}$).

Finally, an experimental investigation of the $4s^2\ {}^1S_0 \rightarrow 4s4p\ {}^1P_1$ Ca resonance transition at 423 nm has been discussed to underline the powerful potential of the novel method. The experimental result impressively demonstrates that this phase-modulated interferometer is well suited for experiments on the realization of novel optical media.

To improve the current phase-shift sensitivity, we will increase the modulation frequency to reduce RIN at the modulation frequency and its harmonics. By balancing the arm length of the interferometer, it will be possible to reduce phase-shift signal noise arising from laser-frequency noise by about 2 orders of magnitude. With decreased technical noise, we will be able to come closer to the shot-noise limit. Then, a shot-noise analysis of the phase-modulated interferometer will be necessary.

Acknowledgements. This work was supported by the SFB 407 of the Deutsche Forschungsgemeinschaft.

References

1. K.-J. Boller, A. Immamoğlu, S.E. Harris: Phys. Rev. Lett. **66**, 2593 (1991); S.-Y. Zhu, M.O. Scully: Phys. Rev. Lett. **76**, 388 (1996); O.A. Kocharovskaya, Y.I. Khanin: Pis'ma Zh. éksp. teor. Fiz. **48**, 581 (1988) (Engl. Transl. JETP Lett. **48**, 6301 (1988)); A. Nottelmann, C. Peters, W. Lange: Phys. Rev. Lett. **70**, 1783 (1993); W.E. van der Veer, R.J.J. van Diest, A. Dönszelmann, H.B. van Linden van den Heuvell: Phys. Rev. Lett. **70**, 3243 (1993); E.S. Fry, X. Li, D.E. Nikonov, G.G. Padmabandu, M.O. Scully, A.V. Smith, F.K. Tittel, C. Wang, S.R. Wilkinson, S.-Y. Zhu: Phys. Rev. Lett. **70**, 3235 (1993)
2. M.O. Scully: Phys. Rev. Lett. **67**, 1855 (1991); M. Xiao, Y.-Q. Li, S.-Z. Jin, J. Gea-Banacloche: Phys. Rev. Lett. **74**, 666 (1995); A.S. Zibrov, M.D. Lukin, L.W. Hollberg, M.O. Scully, H.G. Robinson, V.L. Velichansky: Phys. Rev. Lett. **76**, 3935 (1996); L. v. Hau, S.E. Harris, Z. Duffen, C.H. Behroozi: Nature **397**, 394 (1999)
3. G. Müller, A. Wicht, R.-H. Rinkleff, K. Danzmann: Opt. Commun. **127**, 37 (1996)
4. C. Szymanowski, A. Wicht, K. Danzmann: J. Mod. Opt. **44**, 1373 (1997)
5. M.D. Lukin, P. Hemmer, M. Löffler, M.O. Scully: Phys. Rev. Lett. **81**, 2675 (1998)
6. M.O. Scully, M. Fleischhauer: Phys. Rev. Lett. **69**, 1360 (1992); S. Brandt, A. Nagel, R. Wynands, D. Meschede: Phys. Rev. A **56**, R1063 (1997)
7. A. Wicht, K. Danzmann, M. Fleischhauer, M.O. Scully, G. Müller, R.-H. Rinkleff: Opt. Commun. **134**, 431 (1997)
8. R.W.P. Drever, J.L. Hall, F.V. Kowalski, J. Hough, G.M. Ford, A.J. Munley, H. Ward: Appl. Phys. D **31**, 97 (1983); J. Ye, L.-S. Ma, J.L. Hall: J. Opt. Soc. Am. B **15**, 6 (1998)
9. G.C. Bjorklund: Opt. Lett. **5**, 15 (1980)
10. J.M. Supplee, E.A. Whittaker, W. Lenth: Appl. Opt. **33**, 6294 (1994)
11. N.C. Wong, J.L. Hall: J. Opt. Soc. Am. B **2**, 1527 (1985); J.A. Silver: Appl. Opt. **31**, 707 (1992)
12. L.-G. Wang, D.A. Tate, H. Riris, T.F. Gallagher: J. Opt. Soc. Am. B **6**, 871 (1989); D.R. Hjellme, S. Neegard, E. Vartdal: Opt. Lett. **20**, 1731 (1995)
13. G.R. Janik, C.B. Carlisle, T.F. Gallagher: J. Opt. Soc. Am. B **3**, 1070 (1986)
14. E.S. Polzik, J. Carri, H.J. Kimble: Appl. Phys. B **55**, 279 (1992); F. Marin, A. Bramati, V. Jost, E. Giacobino: Opt. Commun. **140**, 146 (1997); S. Kasapi, S. Lathi, Y. Yamamoto: Opt. Lett. **22**, 478 (1997)
15. T. Yabuzaki, T. Mitsui, U. Tanaka: Phys. Rev. Lett. **67**, 2453 (1991)
16. O. Schmidt, R. Wynands, Z. Hussein, D. Meschede: Phys. Rev. A **53**, R27 (1995)
17. L.D. Landau, E.M. Lifschitz: *Elektrodynamik der Kontinua, Lehrbuch der Theoretischen Physik*, Band 8, 5-te Auflage (Akademie-Verlag, Berlin 1985)
18. Schmidt [16] and co-workers had to use a balanced-input beam splitter in order get rid of the Doppler-induced background signal for the spectroscopic investigations performed on a Cs cell. Hence, it might be desirable to use a balanced-input beam splitter not only for the purpose of better contrast
19. Actually, the exact expression reveals, that imbalance of the beam splitter or of the detector only changes the proportionality constant of the signal but does not introduce an offset at any order
20. H.R. Telle: Spectroch. Acta Rev. **15**, 301 (1993)
21. O.S. Brozek, V. Quetschke, A. Wicht, K. Danzmann: Opt. Commun. **146**, 141 (1998)
22. C.M. Caves: Phys. Rev. D **23**, 1693 (1981)
23. T.M. Niebauer, R. Schilling, K. Danzmann, A. Rüdiger, W. Winkler: Phys. Rev. A **43**, 5022 (1991)
24. For example, see B.L. Schumaker: Opt. Lett. **9**, 189 (1984). It should be emphasized that there is no *strict* equivalence between a quantum description of the balanced homodyne or heterodyne detector used e.g. for squeezing experiments and the interferometer with a balanced detector. This is due to the fact, that in the first case the local oscillator and the signal do commute whereas they do not in the case of the interferometer
25. A. Wicht: Ph. D. Thesis, Universität Hannover, Germany (1998)
26. T. Kisters, K. Zeiske, F. Riehle, J. Helmke: Appl. Phys. B **59**, 89 (1994)
27. A. Witte, T. Kisters, F. Riehle, J. Helmke: J. Opt. Soc. Am. B **9**, 1030 (1992)